Multiple-Symbol-Detection-Based Noncoherent Receivers for Impulse-Radio Ultra-Wideband

Andreas Schenk and Robert F.H. Fischer

Lehrstuhl für Informationsübertragung, Universität Erlangen–Nürnberg, Erlangen, Germany

Email: {schenk,fischer}@lnt.de

Abstract—**Multiple-symbol detection (MSD) is a powerful technique to improve the power efficiency of noncoherent receivers. In this paper, we derive the MSD metric for impulse-radio ultra-wideband for the general case of biorthogonal pulse-position modulation (bPPM) and relate it to its special cases BPSK and PPM. This unified treatment allows us to conduct a comparison of MSD of amplitude- and pulse-position-based impulse-radio signaling schemes in terms of power and spectral efficiency, as well as in terms of complexity.**

I. Introduction

One of the main advantages of the impulse-radio ultra-wideband (IR-UWB) technique in low-complexity transmission systems is its ability to employ noncoherent receivers even in dense multipath propagation scenarios envisioned in typical indoor UWB scenarios [1].

The gap between coherent and noncoherent detection in power efficiency, i.e., in the required signal-to-noise ratio to guarantee a certain bit error rate (BER), can be closed by replacing conventional symbol-by-symbol noncoherent detection with a joint detection of a block of symbols, i.e., performing multiple-symbol detection (MSD). In particular, we consider MSD for differential transmitted reference (DTR) IR-UWB [2], a signaling scheme applying differentially encoded binary phase-shift keying (BPSK). Further considered signaling schemes are orthogonal M-ary pulse-position modulation (M-PPM) [1] and the combination biorthogonal PPM (M-bPPM), i.e., the negatives of the orthogonal PPM signals are included in the signal set, yielding in total $2M$ signal elements. Based on generalized-likelihood ratio testing (GLRT), similar to the approach in [3], we derive the MSD metric of M-bPPM IR-UWB, and relate it to its special cases M-PPM and BPSK.

In [4] these IR-UWB signaling schemes have been compared for transmission over the AWGN channel, while [5] restricts to noncoherent detection of M-PPM in multipath environments. In this paper, we compare the power efficiency of coherent and MSD-based noncoherent receivers for these signaling schemes in a typical UWB multipath propagation scenario. However, only in conjunction with an evaluation of the receiver complexity and the spectral efficiency of the signaling schemes, i.e., the supported number of bits per second per Hertz, we can draw commensurable conclusions from the numerical results. To this end, we evaluate the IR-UWB variants in the power-bandwidth plane [6].

This paper is organized as follows. In Section II, we introduce the system model of M-bPPM IR-UWB used throughout this paper, then derive the MSD metric in Section III, and

relate it to the special cases of M-PPM and BPSK. Section IV compares these signaling schemes via numerical results in terms of power and spectral efficiency, and complexity. We conclude with a summary in Section V.

II. System Model

A. Transmit Signal

The transmit signal of biorthogonal M-ary PPM (M-bPPM) IR-UWB is given as

$$s(t) = \sqrt{E_s/T} \sum_{i=0}^{+\infty} b_i p^{TX}(t - a_i\Delta - iT) \qquad (1)$$

where $a_i \in \mathcal{A} = \{0, ..., M-1\}$ are the PPM information symbols and $b_i \in \mathcal{B} = \{\pm 1\}$ are the differentially encoded information symbols $d_i \in \{\pm 1\}$, i.e., $b_i = b_{i-1}d_i$ and $b_0 = 1$. $p^{TX}(t)$ is the transmit pulse of unit energy and duration $T_{p^{TX}}$ in the order of nanoseconds, Δ is the PPM interval, E_s is the energy per bPPM symbol, and $T = M\Delta$ is the symbol duration. Neglecting the reference for differential encoding, b_0, and assuming i.i.d. equal probable data symbols, each symbol conveys $\log_2(M) + 1$ bits, hence the energy per bit is $E_b = E_s/(\log_2(M) + 1)$. To preclude inter-pulse and inter-symbol interference even in dense multipath environments and allow for multiple-access capability of a large number of simultaneous users, the PPM interval is chosen sufficiently large, i.e., $\Delta = \beta \cdot T_{p^{TX}}$ with $\beta \gg 1$.

B. Spectral Efficiency

Independent of the signaling scheme the transmit signal (1) utilizes a bandwidth approximately proportional to the inverse of the transmit pulse duration, i.e., $\sim \frac{c_p}{T_{p^{TX}}}$, with a constant c_p depending on the specific pulse shape ($c_p \approx \pi$ for the Gaussian monocycle considered later). Hence, the spectral efficiency in bits per second per Hertz of M-bPPM is

$$\Gamma_{\text{bPPM}} = \frac{1 + \log_2(M)}{M} \frac{1}{c_p\beta} \frac{\text{bits/s}}{\text{Hz}} . \qquad (2)$$

C. Receive Signal

Having passed a multipath propagation channel with impulse response $h^{CH}(t)$ and a receive filter $h^{RX}(t)$, the received signal can be written as

$$r(t) = \sum_{i=0}^{+\infty} b_i p(t - a_i\Delta - iT) + n(t) \qquad (3)$$

where $p(t) = \sqrt{E_s/T} \cdot p^{TX}(t) * h^{CH}(t) * h^{RX}(t)$ is the receive pulse shape, and $n(t) = n_0(t) * h^{RX}(t)$ is filtered white Gaussian noise $n_0(t)$ of two-sided power-spectral density $N_0/2$.

D. Coherent Detection

For comparison we recall coherent detection of M-bPPM, assuming ideal knowledge of the receive pulse $p(t)$. For this case, no MSD is necessary and each symbol may be detected by first deciding the transmitted PPM interval based on the magnitude of the crosscorrelation of receive signal and pulse shape, and then the BPSK symbol according to the sign transition in the corresponding interval [6].

III. MULTIPLE-SYMBOL DETECTION

At the receiver MSD is performed, i.e., the transmitted sequences $\boldsymbol{a} \in \mathcal{A}^N$ and $\boldsymbol{b} \in \mathcal{B}^N$ are decided blockwise based on the receive signal in the interval $0 \leq t < NT$ (without loss of generality we consider the interval starting at $t = 0$). The channel is assumed to be constant in this interval, which in typical indoor UWB communication scenarios is fulfilled especially for moderate N [7].

A. Decision Metric

Since the additive noise is Gaussian, we base the joint decision of N information symbols on the log-likelihood metric with respect to a receive signal hypothesis $\tilde{s}(t) = \sum_{i=0}^{N-1} \tilde{b}_i \tilde{p}(t - \tilde{a}_i \Delta - iT)$ corresponding to the trial symbols $\tilde{\boldsymbol{a}} = [\tilde{a}_0, ..., \tilde{a}_{N-1}] \in \mathcal{A}^N$, $\tilde{\boldsymbol{b}} = [\tilde{b}_0, ..., \tilde{b}_{N-1}] \in \mathcal{B}^N$ and a hypothesis $\tilde{p}(t)$ for the unknown receive pulse $p(t)$, both assumed to be of duration $T_\mathrm{I} < \Delta$. Due to the differential encoding the reference sign common to all $\tilde{b}_i$, $i \geq 1$, does not influence the decision metric and may be set to $\tilde{b}_0 = 1$.

Following the GLRT approach [8], in contrast to a maximum-likelihood criterion, we perform an explicit optimization over the unknown receive pulse shape $p(t)$ [3], i.e.,

$$[\hat{\boldsymbol{a}} \ \hat{\boldsymbol{b}}] = \operatorname*{argmax}_{\substack{\tilde{\boldsymbol{a}} \in \mathcal{A}^N, \tilde{\boldsymbol{b}} \in \mathcal{B}^N \\ \tilde{b}_0 = 1}} \max_{\tilde{p}(t)} \int_0^{NT} \left(2 \cdot r(t)\tilde{s}(t) - \tilde{s}^2(t) \right) \, \mathrm{d}t$$

and hence do not draw any assumption on the a-priori probability density function of the multipath arrival times or path gains, apart from the assumed pulse duration T_I. However, this GLRT approach leads to the very same decision metric as the ML-approach in [9], derived based on the assumption of a Gaussian distribution of the channel coefficients and a flat power-delay profile of duration T_I. Hence, under these conditions the GLRT estimate is equal to the ML estimate.

Recalling that both $p(t)$ and its hypothesis are assumed of equal duration T_I and $\tilde{b}_i^2 = 1$, with straightforward calculations, we obtain

$$[\hat{\boldsymbol{a}} \ \hat{\boldsymbol{b}}] = \operatorname*{argmax}_{\substack{\tilde{\boldsymbol{a}} \in \mathcal{A}^N, \tilde{\boldsymbol{b}} \in \mathcal{B}^N \\ \tilde{b}_0 = 1}} \max_{\tilde{p}(t)} \int_0^{T_\mathrm{I}} \left[\tilde{p}(t) \sum_{i=0}^{N-1} \tilde{b}_i r(t + \tilde{a}_i \Delta + iT) \right. \\ \left. - \frac{N}{2} \cdot \tilde{p}^2(t) \right] \, \mathrm{d}t .$$

Similar to [3], fixing $\tilde{\boldsymbol{a}}$ and $\tilde{\boldsymbol{b}}$, we solve the maximization over $\tilde{p}(t)$ analytically using variational calculus (omitted for brevity), and obtain a MSD metric for M-bPPM solely based

on the receive signal in the observation window $0 \leq t < NT$

$$[\hat{\boldsymbol{a}} \ \hat{\boldsymbol{b}}] = \operatorname*{argmax}_{\substack{\tilde{\boldsymbol{a}} \in \mathcal{A}^N, \tilde{\boldsymbol{b}} \in \mathcal{B}^N \\ \tilde{b}_0 = 1}} \int_0^{T_\mathrm{I}} \left[\sum_{i=0}^{N-1} \tilde{b}_i r(t + \tilde{a}_i \Delta + iT) \right]^2 \, \mathrm{d}t . \tag{4}$$

The assumed receive pulse duration T_I, the integration interval, should be set on the one hand large enough to capture sufficient energy of the receive signal, and on the other hand as small as possible not to accumulate too much noise.

Solving (4) requires finding the maximum of $2^{N-1} M^N$ combinations of weighted receive signal intervals, hence, only moderate values of N seem to be applicable. For sufficiently high sampling frequency, (4) can straightforwardly be formulated to work on the sampled and quantized receive signal, analog delay lines can hence be avoided [9]. Implicit restrictions on the sequences $\boldsymbol{a}$ and $\boldsymbol{b}$, as, e.g., in DTR signaling, can be used to reduce the number of candidates, yet, this is not considered here.

Due to the differential encoding, $N = 1$ does not lead to reasonable performance. However, a natural way to overcome this is to perform symbol-by-symbol energy detection (ED) of the M-PPM part ($N = 1$) and differential detection (DD) of the BPSK part ($N = 2$).

B. PPM

The special case of MSD of M-PPM IR-UWB results by setting $b_i = 1$, $\forall i$ (each symbol now conveys $\log_2(M)$ bits, hence $E_\mathrm{b} = E_\mathrm{s} / \log_2(M)$), and the corresponding MSD metric is given as

$$\hat{\boldsymbol{a}} = \operatorname*{argmax}_{\tilde{\boldsymbol{a}} \in \mathcal{A}^N} \int_0^{T_\mathrm{I}} \left[\sum_{i=0}^{N-1} r(t + \tilde{a}_i \Delta + iT) \right]^2 \, \mathrm{d}t . \tag{5}$$

If $N = 1$, (5) corresponds to ED of M-PPM.

C. BPSK

Similarly, MSD of a solely BPSK modulated signal can be viewed as a special case of MSD of M-bPPM. Setting $M = 1$ ($\mathcal{A} = \{0\}$), each symbol represents a single bit, hence $E_\mathrm{b} = E_\mathrm{s}$. Note that b_i still are the differentially encoded information symbols. Using $\tilde{b}_i^2 = 1$, the corresponding MSD metric can be rearranged [3], yielding the triangular structure

$$\hat{\boldsymbol{b}} = \operatorname*{argmax}_{\substack{\tilde{\boldsymbol{b}} \in \mathcal{B}^N \\ \tilde{b}_0 = 1}} \sum_{i=1}^{N-1} \sum_{j=0}^{i-1} \tilde{b}_i \tilde{b}_j \int_0^{T_\mathrm{I}} r(t + iT) r(t + jT) \, \mathrm{d}t . \tag{6}$$

Hence, for the special case of BPSK signaling the MSD metric in (4) reduces to an autocorrelation of the receive signal with delays being multiples of the symbol duration T, followed by maximization of the decision metric, as shown in [2], [3]. The latter can be formulated as a tree search problem and is efficiently implemented by the sphere decoder (SD), which avoids testing all 2^{N-1} candidate sequences (complexity exponential in N), resulting in effectively polynomial search complexity for a wide range of signal-to-noise ratios. Thus considerably larger MSD window lengths N compared to a full search as required for MSD of PPM become amenable [3], [10].
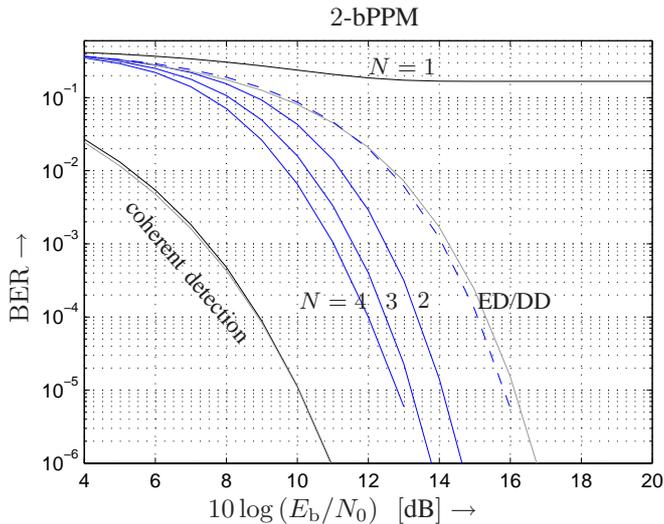
Fig. 1. BER vs. E_b/N_0 in dB for MSD of 2-bPPM IR-UWB with different N in comparison to conventional ED ($N = 1$), coherent detection, and ED/DD detection (dashed). Gray lines: analytical/approximate BER.
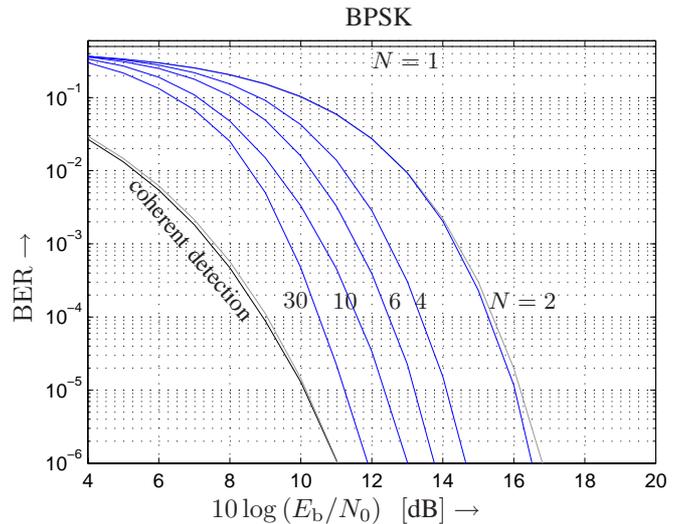

Fig. 3. BER vs. E_b/N_0 in dB for MSD of BPSK IR-UWB with different N in comparison to conventional ED ($N = 1$), DD ($N = 2$) and coherent detection. Gray lines: analytical/approximate BER.
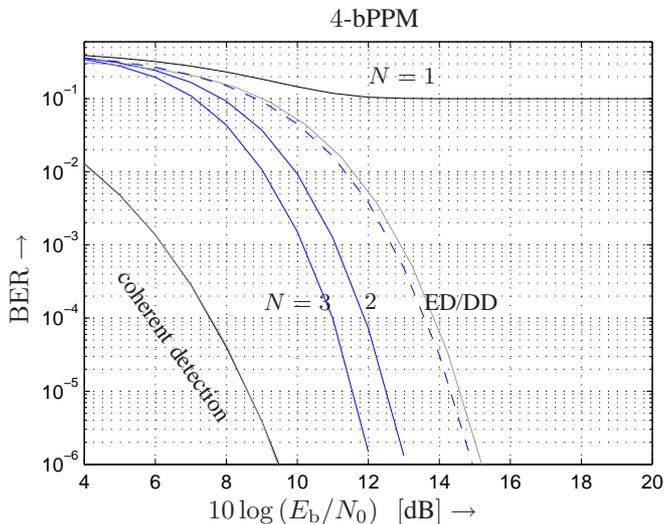

Fig. 2. BER vs. E_b/N_0 in dB for MSD of 4-bPPM IR-UWB with different N in comparison to conventional ED ($N = 1$), coherent detection, and ED/DD detection (dashed). Gray lines: analytical/approximate BER.
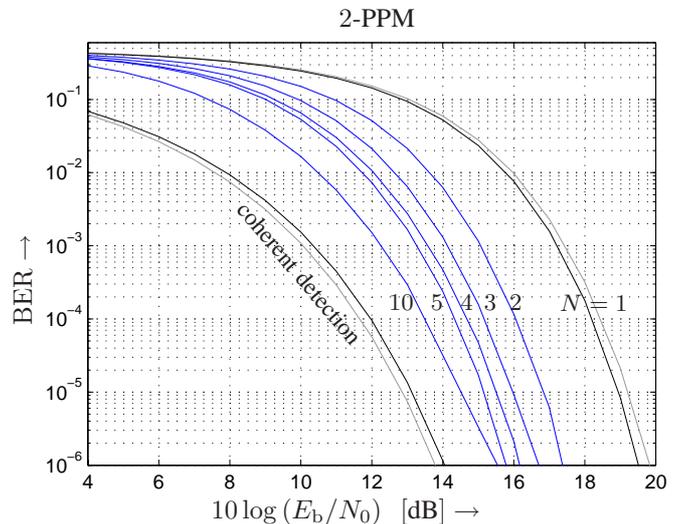

Fig. 4. BER vs. E_b/N_0 in dB for MSD of 2-PPM IR-UWB with different N in comparison to conventional ED ($N = 1$) and coherent detection. Gray lines: analytical/approximate BER.

In a similar way, MSD of M-bPPM can be realized with M^N parallel autocorrelation receivers, each tuned to one PPM sequence followed by a SD to find the corresponding BPSK part. This puts most of the receiver complexity on detection of the PPM part, while the BPSK part is decided with little additional effort.

IV. COMPARISON

We compare MSD of the various signaling schemes via numerical results in a typical UWB scenario, where we assume no inter-symbol interference (T chosen sufficiently large), $T_{p^{TX}} = 1\,\mathrm{ns}$, and $p^{TX}(t)$ is a Gaussian monocycle with $10\,\mathrm{dB}$ bandwidth of $3.3\,\mathrm{GHz}$ and $2.25\,\mathrm{GHz}$ center frequency. The propagation channel is modeled according to IEEE-CM 2 [7] with each realization normalized to unit energy. The receive filter is modeled as an ideal $3\,\mathrm{GHz}$ bandpass filter around

the pulse center frequency and a good compromise for the integration time is $T_I = 30\,\mathrm{ns}$.

In all figures, gray lines represent approximate BER expressions of ED/DD, which directly result from a Gaussian approximation of the decision metric in the spirit of [2], [11], [12], and the analytical BER for the well known case of coherent detection [6] (omitted here due to lack of space).

Exemplary, Figure 1 and Figure 2 depict the BER of MSD of 2 and 4-bPPM IR-UWB, respectively. The dashed line corresponds to the low-complexity detection (see Section III), i.e., symbol-by-symbol ED of the PPM part followed by DD of the BPSK part. Already MSD with $N = 2$ leads to a gain of $2\,\mathrm{dB}$ in comparison to ED/DD at BER $= 10^{-5}$. With increasing N performance is improved further and approaches that of coherent detection.

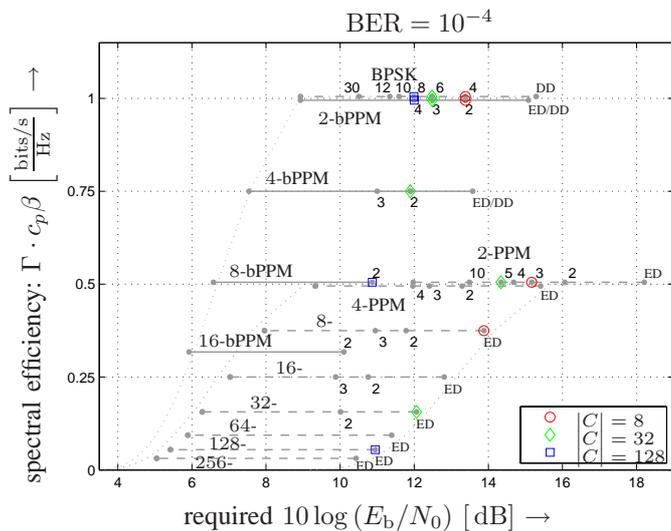Turning to BPSK, MSD using the SD however enables

Fig. 5. Trade-off power vs. spectral efficiency at BER $= 10^{-4}$ of IR-UWB coherent detection and MSD with parameter N as indicated. Solid lines: M-bPPM, dashed: M-PPM, dash-dotted: BPSK. Colored markers: MSD with an equal number of candidates. Dotted lines: analytical/approximate BER.

considerably larger N in the order of 30 and results in performance close to coherent detection ($1\,\mathrm{dB}$ difference for $N = 30$ at BER $= 10^{-5}$), as depicted in Figure 3. Here $N = 2$ corresponds to conventional autocorrelation DD.

Considering 2-PPM, from Figure 4 it can be seen, that again already the joint decision of two 2-PPM symbols leads to a gain of more than $2\,\mathrm{dB}$ compared to conventional ED. Larger N bridge the gap to coherent detection of 2-PPM with ideal knowledge of the receive pulse shape. In comparison to 2-bPPM, for a fixed N 2-PPM shows a loss of approximately $3\,\mathrm{dB}$, indicating that the PPM part dominates the bPPM performance.

For the same setting as above, Figure 5 visualizes the trade-off between power and spectral efficiency (see (2)) of the studied signaling schemes at BER $= 10^{-4}$. The lines are parameterized by the MSD window parameter N (indicated next to the dots), where the left most dot corresponds to coherent detection and the right most dot to DD ($N = 2$) for BPSK, to the low-complexity detection as described in Section III (termed ED/DD) for M-bPPM, and to ED ($N = 1$) for M-PPM. Dotted lines represent the performance resulting from analytical/approximate BER expressions. Markers flag an equal number of candidate sequences required for MSD (indicating the receiver complexity–further complexity reduction due to the application of the SD for MSD of BPSK may be possible).

The gain achieved by increasing the MSD window N, naturally accompanied with an increase in receiver complexity, is similar to all the signaling schemes. However, it is important to note that signaling schemes making use of the sign information of the pulse, i.e., BPSK and M-bPPM, lead to a significant increase both in power and in spectral efficiency in comparison to the solely pulse-position-based scheme M-PPM.

Fixing the number of candidate sequences in MSD, i.e., the dimensionality of the search problem (M-bPPM: $2^{N-1}M^N$, BPSK: 2^{N-1}, M-PPM: M^N), from the markers in Figure 5 it can be seen that under this constraint BPSK and 2-bPPM, both

signaling schemes using the sign of the pulse, achieve very similar power efficiency, which is substantially higher than that of 2-PPM. Only higher-order PPM overcomes this drawback, however, at the cost of considerably reduced spectral efficiency. This extends the well-known fact for coherent detection [6] and the conclusions of [4] to the case of MSD-based noncoherent detection of IR-UWB in multipath propagation scenarios.

Note that the significant complexity reduction achieved with the application of the SD in MSD of BPSK (and similar in M-bPPM) is not mirrored in Figure 5. The advantages of BPSK and M-bPPM in terms of power and spectral efficiency are accompanied by a reduction in the complexity of noncoherent receivers, which further substantiates to favor sign-based schemes, i.e., BPSK or M-bPPM, over pulse-position-based schemes in IR-UWB systems.

V. CONCLUSIONS

In this paper we have compared MSD-based noncoherent receivers for IR-UWB using BPSK, PPM, and biorthogonal PPM with respect to performance, complexity, and spectral efficiency. To this end, we derived the MSD decision metric of biorthogonal PPM IR-UWB and related it to its special cases of PPM and BPSK. While the gain achieved with increasing MSD block length is similar for all IR-UWB signaling schemes, making use of the sign information, i.e., BPSK and biorthogonal PPM, proves preferable to solely PPM not only in terms of power and spectral efficiency, but also in terms of complexity.

REFERENCES

[1] M. Z. Win and R. A. Scholtz, "Impulse Radio: How It Works," *IEEE Commun. Lett.*, vol. 2, no. 2, pp. 36–38, Feb. 1998.

[2] N. Guo and R. C. Qiu, "Improved Autocorrelation Demodulation Receivers Based on Multiple-Symbol Detection for UWB Communications," *IEEE Trans. Wireless Commun.*, vol. 5, no. 8, pp. 2026–2031, Aug. 2006.

[3] V. Lottici and Z. Tian, "Multiple Symbol Differential Detection for UWB Communications," *IEEE Trans. Wireless Commun.*, vol. 7, no. 5, pp. 1656–1666, May 2008.

[4] H. Zhang and T. A. Gulliver, "Biorthogonal Pulse Position Modulation for Time-Hopping Multiple Access UWB Communications," *IEEE Trans. Wireless Commun.*, vol. 4, no. 3, pp. 1154–1162, May 2005.

[5] Y. Souilmi and R. Knopp, "On the Achievable Rates of Ultra-Wideband PPM with Non-Coherent Detection in Multipath Environments," in *Proc. IEEE International Conference on Communications (ICC '03)*, vol. 5, pp. 3530–3534, Anchorage, USA, May 11–15, 2003.

[6] J. G. Proakis and M. Salehi, *Digital Communications*, 5th ed. New York, NY, USA: McGraw-Hill, 2008.

[7] A. F. Molisch, J. R. Foerster, and M. Pendergrass, "Channel Models for Ultrawideband Personal Area Networks," *IEEE Wireless Commun. Mag.*, vol. 10, no. 6, pp. 14–21, Dec. 2003.

[8] S. M. Kay, *Fundamentals of Statistical Signal Processing: Volume II - Detection Theory*. New Jersey, USA: Prentice-Hall PTR, 1998.

[9] Y. Tian and C. Yang, "Noncoherent Multiple-Symbol Detection in Coded Ultra-Wideband Communications," *IEEE Trans. Wireless Commun.*, vol. 7, no. 6, pp. 2202–2211, Jun. 2008.

[10] A. Schenk, R. F. H. Fischer, and L. Lampe, "A New Stopping Criterion for the Sphere Decoder in UWB Impulse-Radio Multiple-Symbol Differential Detection," in *Proc. IEEE International Conference on Ultra-Wideband (ICUWB '09)*, pp. 589–594, Vancouver, Canada, Sep. 9–11, 2009.

[11] T. Q. S. Quek and M. Z. Win, "Analysis of UWB Transmitted-Reference Communication Systems in Dense Multipath Channels," *IEEE J. Sel. Areas Commun.*, vol. 23, no. 9, pp. 1863–1874, Sep. 2005.

[12] M. Pausini and G. J. M. Janssen, "Performance Analysis of UWB Autocorrelation Receivers Over Nakagami-Fading Channels," *IEEE J. Sel. Topics Signal Process.*, vol. 1, no. 3, pp. 443–455, Oct. 2007.